Optical Sideband Generation: a Longitudinal Electron Beam Diagnostic Beyond the Laser Bandwidth Resolution Limit

J. van Tilborg, N. H. Matlis, G. R. Plateau and W. P. Leemans

Lawrence Berkeley National Laboratory, University of California, Berkeley, California 94720, USA

Abstract. Electro-optic sampling (EOS) is widely used as a technique to measure THz-domain electric field pulses such as the self-fields of femtosecond electron beams. We present an EOS-based approach for single-shot spectral measurement that excels in simplicity (compatible with fiber integration) and bandwidth coverage (overcomes the laser bandwidth limitation), allowing few-fs electron beams or single-cycle THz pulses to be characterized with conventional picosecond probes. It is shown that the EOS-induced optical sidebands on the narrow-bandwidth optical probe are spectrally-shifted replicas of the THz pulse. An experimental demonstration on a 0-3 THz source is presented.

Keywords: Beam diagnostics, electro-optic sampling, ultra-short electron beams
PACS: 230.2090, 300.6495, 320.2250, 320.7100

INTRODUCTION

Control and measurement of terahertz (THz) pulses allow scientists to unravel ultra-fast phenomena in plasmas, semiconductors, and superconductors. The method of laser-based electro-optic sampling (EOS) [1, 2] has proven a powerful technique for characterizing single-cycle broad-bandwidth THz radiation [3]. EOS also serves as a single-shot temporal diagnostic for femtosecond accelerator-produced electron bunches [4]. Conventional single-shot EOS-based techniques measure the modified optical pulse in the temporal [3, 4], spatial [5], or spectral domain [6]. Here the temporal resolution and corresponding covered THz bandwidth is determined by the probe laser bandwidth. Although few-fs few-cycle probe pulses (~100 THz bandwidth coverage) have been applied in multi-shot EOS configurations [7], single-shot measurements are limited to longer >40-fs-type probe beams due to challenges in laser technology and user friendliness. For state-of-the-art single-cycle electromagnetic sources and electron accelerators moving into the few-femtosecond domain, this single-shot laser-bandwidth limit needs to be overcome. Here we introduce and experimentally demonstrate a novel EOS configuration based on THz-induced optical sideband generation (analogous to THz-induced sidebands in semiconductor systems [8, 9]). This single-shot technique excels in simplicity (compatible with fiber integration) and measures the THz pulse spectrum with a bandwidth coverage corresponding to a few-fs (or shorter) temporal resolution.

EOS can be understood [2] as nonlinear mixing, in an electro-optic (EO) crystal, of the THz frequency components at Ω with the optical field components at ω to produce new optical components at the sum and difference frequencies $\omega \pm \Omega$. Ω and ω represent angular frequencies. In conventional EOS techniques the optical spectrum of the probe pulse is typically broad-band, extending well past the EOS-induced components $\omega \pm \Omega$, such that the new and existing optical contributions add up coherently and appear as an amplitude or phase shift. Relying on a broad-band probe laser limits the THz coverage to the probe laser bandwidth. Here we circumvent this limit by concentrating on the optical sidebands created outside the probe laser's (narrow) bandwidth.

THEORETICAL CONCEPTS

The basic concept of the sideband generation scheme is shown in Fig. 1(a). An optical probe pulse is focused onto an EO crystal. In the spectral domain, the electric field of this optical pulse can be defined as $E_{\mathrm{opt}}(\omega) = E_0 \exp\left[-(\omega-\omega_0)^2/\sigma_\omega^2\right]$ with E_0 the spectral amplitude and σ_ω the optical bandwidth [with corresponding temporal intensity full-width-at-half-maximum (FWHM) $2.35/\sigma_\omega$]. Also incident on the EO crystal is either [in the THz radiation mode, see Fig. 1(a)] a focused electromagnetic THz pulse with field $E_{\mathrm{THz}}(\Omega)$ or [in the electron beam mode, see Fig. 1(b)] the self-fields of a femtosecond electron beam with charge profile $Q(t)$, whose Fourier transform yields a THz-domain field spectrum of $E_{\mathrm{THz}}(\Omega) \sim \int dt Q(t) \exp(-\imath\Omega t)$. Figures 1(c) and 1(d) show example THz

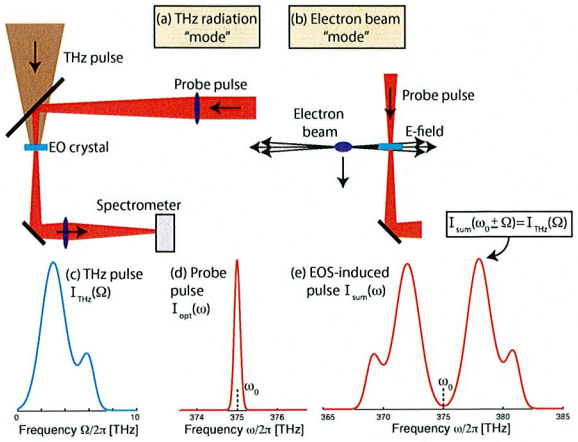

FIGURE 1. (color online) Schematic concept for optical sideband generation as a THz pulse diagnostic. (a) Incident on the EO crystal is both an electromagnetic THz pulse and an optical probe pulse. (b) In the electron beam mode the THz pulse represents the transverse electric field of a femtosecond electron bunch. (c, d) Example THz pulse spectrum $I_{\mathrm{THz}}(\Omega)$ and narrow-bandwidth probe pulse spectrum $I_{\mathrm{opt}}(\omega)$, respectively. (e) EOS-induced optical spectrum $I_{\mathrm{sum}}(\omega)$ based on EO mixing of the waveforms from (c) and (d). Assuming $I_{\mathrm{THz}}(\Omega) = I_{\mathrm{THz}}(-\Omega)$, it can be seen that $I_{\mathrm{sum}}(\omega_0 \pm \Omega) \simeq I_{\mathrm{THz}}(\Omega)$.

and probe pulse spectra, respectively. Following the approach by Jamison *et al.* [2, 10], the frequency mixing inside the EO crystal leads to sum and difference frequency generation (labeled as E_{sum}). In a coordinate system where the induced two-photon polarization P and input optical field E_{opt} are parallel, the nonlinear polarization can be expressed as $P = \varepsilon_0 \chi^{(2)}_{\mathrm{eff}} E_{\mathrm{THz}} E_{\mathrm{opt}}$, with $\chi^{(2)}_{\mathrm{eff}}$ the effective electro-optic parameter. Applying the slowly varying envelope approximation to the optical field envelopes, Jamison *et al.* [2] showed that the solution to the wave equation can be rewritten as

$$E_{\mathrm{sum}}(\omega) = \frac{L\omega}{c n_{\mathrm{opt}}} \phi_0 \int_{-\infty}^{\infty} d\Omega T_{\mathrm{cr}}(\Omega) E_{\mathrm{THz}}(\Omega) E_{\mathrm{opt}}(\omega - \Omega), \tag{1}$$

with $T_{\mathrm{cr}}(\Omega)$ the crystal transfer function, L the crystal thickness, n_{opt} the crystal index of refraction at ω_0, and ϕ_0 a unitary factor given by $\left[\imath \exp\left(-\beta L + \imath \omega n_{\mathrm{opt}} L/c\right)\right]$ with c the light speed in vacuum, and β the optical absorption in the EO crystal. Equation (1) describes the optical sideband generation for arbitrary THz pulses, including arbitrary spectral phase. A further simplification to Eq. (1) can be made if we can assume that the probe laser amplitude is constant over the duration T_{THz} of the THz pulse ($T_{\mathrm{THz}} \ll 1/\sigma_\omega$). Under these conditions, the integral in Eq. (1) is only nonzero around $\Omega \simeq |\omega - \omega_0|$ and Eq. (1) can be simplified as

$$E_{\mathrm{sum}}(\omega_0 \pm \Omega) = \frac{(\omega_0 \pm \Omega) L}{c n_{\mathrm{opt}}} \phi_0 E_0 \sigma_\omega \sqrt{\pi} T_{\mathrm{cr}}(\Omega) E_{\mathrm{THz}}(\Omega). \tag{2}$$

Equation (2) shows that the crystal-modulated THz spectrum is now represented in the optical domain. Based on the example THz and probe spectra of Figs. 1(c) and 1(d), the modeled optical intensity $I_{\mathrm{sum}}(\omega)$ is shown in Fig. 1(e). The crystal transfer function was simplified here to be a constant. One can see that the optical spectrum $I_{\mathrm{sum}}(\omega)$ is a direct match to the ω_0-shifted THz pulse spectrum. While Eq. (2) predicts that the sideband field amplitude is linearly proportional to σ_ω, the spectral resolution of this THz retrieval method is also linear with σ_ω. For example, in order to resolve sharp THz spectral features such as a $(2\pi \cdot 40)$-GHz-width absorption line, an upper boundary to the laser bandwidth of $\sigma_\omega = 2\pi \cdot 40$ GHz (equivalent to a temporal intensity FWHM of 9.4 ps) is required.

Equations (1) and (2) indicate that the crystal transfer function $T_{\mathrm{cr}}(\Omega)$ [11] will affect the THz pulse retrieval from the measured sideband spectrum. $T_{\mathrm{cr}}(\Omega)$ incorporates the frequency dependent EO parameter $\chi^{(2)}_{\mathrm{eff}}(\Omega)$ [12], the effect of Fabry-Perot reflections of the THz pulse inside the crystal, and the phase-matching function [2] which incorporates THz absorption, dispersion, and velocity walk-off between optical and THz fields. $T_{\mathrm{cr}}(\Omega)$ can either be measured and calibrated, or retrieved from the literature. Note that to cover a THz bandwidth in excess of 50 THz, ultra-thin EO crystals (at the cost of signal strength) such as 5-μm-thick GaSe could be employed.

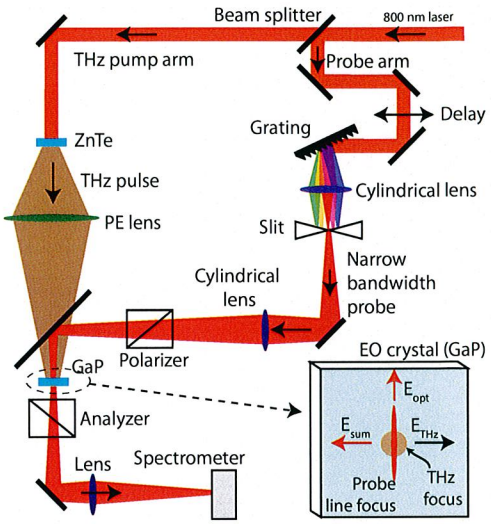

FIGURE 2. (color online) Experimental setup for the THz-induced optical sideband diagnostic. A laser beam is split by a beam splitter into two arms, namely a pump arm for THz generation and a probe arm. The THz pulse is focused by a polyethylene (PE) lens onto an EO crystal. The probe arm is reflected off a grating-lens-slit combination to produce a narrow bandwidth probe pulse $E_{\text{opt}}(\omega)$ onto the EO crystal, after which an imaging spectrometer records the spectrum $I_{\text{sum}}(\omega)$. The inset at the bottom right shows a schematic of the spatial profiles of the THz pulse and probe beam, as well as the relevant polarization vectors.

EXPERIMENTAL DEMONSTRATION

In order to experimentally demonstrate the diagnostic capability of THz-induced optical sideband production, we developed a laser-based THz generation setup delivering both a THz pulse and a narrow-bandwidth probe beam onto a GaP crystal. The laser was based on a 1-kHz Titanium-sapphire laser system ($\lambda_0 = 800$ nm) as depicted in Fig. 2. A collimated laser pulse with a 3.1 mm intensity FWHM and 35 fs temporal FWHM was incident onto a beam splitter (top right). The vertically-polarized transmitted beam (labeled as THz pump beam), at an energy of 510 μJ /pulse, was propagated onto a 200-μm-thick ZnTe crystal for production of THz radiation through optical rectification [13]. The horizontally-polarized THz pulse (see [13] for polarization details) was focused by a 60-mm-focal-length polyethylene lens (transmission limited to 0-3 THz) through a thin nitro-cellulose dielectric-coated pellicle onto a 200-μm-thick GaP crystal for EO detection.

We chose to derive the narrow-bandwidth probe beam from the THz-pump laser line to guarantee temporal synchronization. As illustrated in Fig. 2, the probe beam from the beam splitter (60 μJ/pulse) was sent through a delay stage onto a 600 lines/mm grating to accomplish spectral dispersion. A cylindrical lens placed after the grating produced a line focus, with each color focused to a different position. A 150-μm slit was placed in the focal plane of the lens, therefore only transmitting a narrow controllable part of the optical bandwidth. By imaging the slit onto the GaP crystal (one-to-one imaging) and imaging the crystal plane onto the 300-μm opening slit of a 0.25-m 14-bit 1-Mpixel-CCD imaging spectrometer, we were able to record two-dimensional (wavelength and space) optical spectra with a calibration of 0.23 nm/pixel horizontally and 42 μm/pixel vertically. By carefully selecting the proper EO crystal axis rotation as well as the polarization vectors of the optical and THz beams, we were able to operate in the polarization extinction mode. In this mode, the optical spectrum of the input beam $I_{\text{opt}}(\omega)$ was rejected by the analyzer (with extinction efficiency of $1.4 \cdot 10^{-4}$), while the EOS-induced optical spectrum $I_{\text{sum}}(\omega)$ was transmitted by the analyzer. Note that remnant $I_{\text{opt}}(\omega)$ still frustrated THz retrieval at frequencies $\Omega < \sigma_\omega$.

An image of the measured optical spectrum with the THz beam blocked is shown in Fig. 3(a). Although the demonstrated technique has single-shot capabilities, the images in Fig. 3 represent an accumulation of 500 laser shots for improved signal-to-noise. Figure 3(b) shows the spectrometer image with the THz beam unblocked. A line-out through the center of the THz spot is shown in Fig. 3(c), where the frequency axis was set by shifting the original spectral axis by $\omega_0/(2\pi) = 375$ THz. As predicted, the THz spectrum appears as symmetric sidebands in the optical domain. It was verified that the measured spectrum in Fig. 3(c) is in qualitative agreement with theoretical predictions

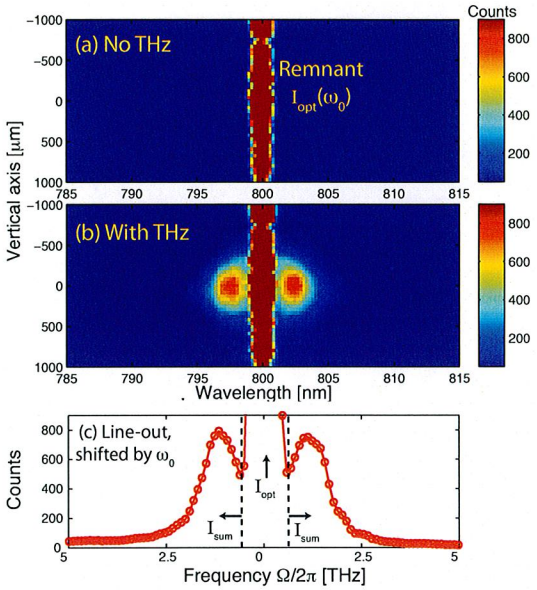

FIGURE 3. (color online) (a) Spectrometer image obtained with no THz field present. Remnant laser radiation of the probe beam around 800 nm is still observed. (b) Image of THz-induced optical sidebands with the on-axis line-out shown in (c). For the latter, the spectrum was shifted by $\omega_0/(2\pi)$ =375 THz. The optical sidebands are replicas of the THz pulse spectrum incident on the GaP crystal.

(dominated by PE transmission).

Note that for single-cycle THz pulses or 50-pC-type femtosecond electron beams (with peak fields on the order of 0.1-10 MV/cm), signal ratios $I_{\rm sum}(\omega)/I_{\rm opt}(\omega_0)$ on the order of $\sim 10^{-9} - 10^{-5}$ are expected. Such ratio requires a combination of significant probe energy, a sensitive spectrometer, and polarization extinction of $I_{\rm opt}(\omega_0)$. Details on signal-to-noise optimization will be addressed in future work.

CONCLUSION

In conclusion, we have presented the concept of THz-induced optical sideband generation as a single-shot THz pulse diagnostic. The technique can be applied to electromagnetic THz radiation as well as to the self-fields of femtosecond electron bunches. The novel approach is not effected by laser bandwidth limitations, enabling large spectral coverage (>60 THz) from few-fs electron beams. Potential fiber integration of the setup offers advantages in user friendliness. We have experimentally demonstrated the diagnostic by observing optical sidebands from a 0-3 THz laser-based source.

ACKNOWLEDGMENTS

The authors gratefully acknowledge contributions from A. J. Gonsalves, J. Osterhoff, Cs. Tóth, and R. A. Kaindl. This work was supported by the Director, Office of Science, Office of High Energy Physics, of the U.S. Department of Energy under Contract No. DE-AC02-05CH11231.

REFERENCES

1. G. Gallot, and D. Grischkowsky, J. Opt. Soc. Am. B **16**, 1204 (1999).
2. S. P. Jamison, A. M. MacLeod, B. Berden, D. A. Jaroszynski, and W. A. Gillespie, Opt. Lett. **31**, 1753 (2006).

3. J. van Tilborg, Cs. Tóth, N. H. Matlis, G. R. Plateau, and W. P. Leemans, Opt. Lett. **32**, 313 (2007).
4. G. Berden, S. P. Jamison, A. M. MacLeod, W. A. Gillespie, B. Redlich, and A. F. G. van der Meer, Phys. Rev. Lett. **93**, 114802 (2004).
5. J. Shan, A. S. Weling, E. Knoesel, L. Bartels, M. Bonn, A. Nahata, G. A. Reider, and T. F. Heinz, Opt. Lett. **25**, 426 (2000).
6. N. H. Matlis, G. R. Plateau, J. van Tilborg, and W. P. Leemans, J. Opt. Soc. Am. B, accepted.
7. A. Sell, R. Scheu, A. Leitenstorfer, and R. Huber, Appl. Phys. Lett. **93**, 251107 (2008).
8. M. A. Zudov, J. Kono, A. P. Mitchell, and A. H. Chin, Phys. Rev. B **64**, 121204R (2001).
9. V. Ciulin, S. G. Carter, M. S. Sherwin, A. Huntington, and L. A. Coldren. Phys. Rev. B **70**, 115312 (2004).
10. S. P. Jamison, Appl. Phys. B **91**, 241 (2008).
11. J. Faure, J. van Tilborg, R. A. Kaindl, and W. P. Leemans, Opt. Quantum Electron. **36**, 681–697 (2004).
12. A. Leitenstorfer, S. Hunsche, J. Shah, M. C. Nuss, and W. H. Knox, Appl. Phys. Lett. **74**, 1516 (1999).
13. Q. Chen, M. Tani, Z. Jiang, and X. -C. Zhang, J. Opt. Soc. Am. B **18**, 823 (2010).

DISCLAIMER